Gating of Maxi K$^+$ Channels Studied by Ca^{2+} Concentration Jumps in Excised Inside-out Multi-Channel Patches (Myocytes from Guinea Pig Urinary Bladder)

F. MARKWARDT and G. ISENBERG

From the Department of Physiology, University of Cologne, 5000 Cologne 41, Germany

ABSTRACT   Currents through maxi K$^+$ channels were recorded in inside-out macro-patches. Using a liquid filament switch (Franke, C., H. Hatt, and J. Dudel. 1987. *Neurosci. Lett.* 77:199–204) the Ca^{2+} concentration at the tip of the patch electrode ([Ca^{2+}]$_i$) was changed in <1 ms. Elevation of [Ca^{2+}]$_i$ from <10 nM to 3, 6, 20, 50, 320, or 1,000 μM activated several maxi K$^+$ channels in the patch, whereas return to <10 nM deactivated them. The time course of Ca^{2+}-dependent activation and deactivation was evaluated from the mean of 10–50 sweeps. The mean currents started with a ~10-ms delay that was attributed to diffusion of Ca^{2+} from the tip to the K$^+$ channel protein. The activation and deactivation time courses were fitted with the third power of exponential terms. The rate of activation increased with higher [Ca^{2+}]$_i$ and with more positive potentials. The rate of deactivation was independent of preceding [Ca^{2+}]$_i$ and was reduced at more positive potentials. The rate of deactivation was measured at five temperatures between 16 and 37°C; fitting the results with the Arrhenius equation yielded an energy barrier of 16 kcal/mol for the Ca^{2+} dissociation at 0 mV. After 200 ms, the time-dependent processes were in a steady state, i.e., there was no sign of inactivation. In the steady state (200 ms), the dependence of channel openness, $N \cdot P_o$, on [Ca^{2+}]$_i$ yielded a Hill coefficient of ~3. The apparent dissociation constant, K_D, decreased from 13 μM at −50 mV to 0.5 μM at +70 mV. The dependence of $N \cdot P_o$ on voltage followed a Boltzmann distribution with a maximal P_o of 0.8 and a slope factor of ~39 mV. The results were summarized by a model describing Ca^{2+}- and voltage-dependent activation and deactivation, as well as steady-state open probability by the binding of Ca^{2+} to three equal and independent sites within the electrical field of the membrane at an electrical distance of 0.31 from the cytoplasmic side.

Address reprint requests to Dr. G. Isenberg, Department of Physiology, University of Cologne, 5000 Cologne 41, Germany.

F. Markwardt's permanent address is Department of Physiology, Martin-Luther-University Halle/S., Leninallee 6, 4010 Halle/S., Germany.

INTRODUCTION

Ca^{2+}-activated maxi K^+ channels with conductances of > 100 pS have been described in many cells. Because of their fast activation by depolarization or by an increase in cytosolic calcium concentration ($[Ca^{2+}]_i$), they are thought to carry outward currents that serve to repolarize the action potential (for references, see Latorre, Coronado, and Vergara, 1984). For the sustained changes in $[Ca^{2+}]_i$ there are numerous single channel analyses that have yielded detailed models with several open and closed conformations. Despite this knowledge, the discussion of whether Ca^{2+} binding is voltage dependent and rate limiting for the time course of activation is still controversial (Methfessel and Boheim, 1982; Magleby and Pallotta, 1983a, b; Moczydlowski and Latorre, 1983; Latorre et al., 1984; McManus and Magleby, 1989).

This controversy is partially due to a scarcity of experiments analyzing the time course of Ca^{2+}-dependent activation and deactivation. In this study, this information was obtained from analyzing mean currents through Ca^{2+}-activated K^+ channels in inside-out macro-patches that were exposed to fast (millisecond range) Ca^{2+} concentration jumps ("liquid filament switch," Franke, Hatt, and Dudel, 1987). In the plasma membrane of urinary bladder myocytes, the channels are grouped in clusters of more than two, making single channel analysis almost impossible. The situation, however, is well suited for studying the time course by mean currents obtained from 10–50 individual sweeps. The relaxation kinetics of these mean currents upon sudden $[Ca^{2+}]_i$ jumps provided clear evidence that a jump in Ca^{2+} concentration activates the channel within milliseconds and that the activation time course is rate limited by the binding of Ca^{2+}. The results were consistent with a model describing Ca^{2+}- and voltage-dependent activation, deactivation, and open probability by the binding of Ca^{2+} to three equal and independent binding sites within the electrical field of the membrane.

Some of the results have been previously reported in abstract form (Markwardt and Isenberg, 1990, 1991).

MATERIALS AND METHODS

Myocytes were isolated enzymatically from the urinary bladder of 300-g guinea pigs according to the method of Klöckner and Isenberg (1985). The isolated cells were stored at 4°C in a "KB medium" (Isenberg and Klöckner, 1982) composed of (mM): 60 KCl, 30 K_2HPO_4, 1 EGTA, 5 $MgCl_2$, 5 K-pyruvate, 5 creatine, 20 taurine, 20 glucose, 5 succinic acid, 5 glutamic acid, and 1 g/liter fatty acid free albumin, adjusted with ~40 mM KOH to a pH of 7.2. A drop of KB medium containing the cell suspension was placed in the experimental chamber (volume ~0.1 ml). After the cells had settled down, the chamber was perfused at a rate of ~5 ml/min with a physiological salt solution (PSS) composed of (mM): 150 NaCl, 5.4 KCl, 1.2 $MgCl_2$, 0.2 $CaCl_2$, 20 glucose, and 5 HEPES, adjusted with NaOH to pH 7.4.

Patch pipettes (5–20 $M\Omega$) were filled with a solution containing (mM): 150 KCl, 1 $MgCl_2$, and 10 HEPES, adjusted with KOH to pH 7.2. After a high resistance seal had formed (5–30 $G\Omega$), the patch was excised and positioned ~5 μm from the border of a liquid filament. The filament was the laminar stream of solution flowing out of the glass pipette in the same direction as the bath perfusion. The filament solution was composed of (mM): 150 KCl, 1 EGTA, and 10 HEPES, adjusted with KOH to pH 7.4. The filament glass pipette was mounted to a piezo ceramic (Physik Instrumente, Waldbronn, Germany). Computer-controlled application of 80-V

pulses shifted the filament by ~20 μm perpendicular to the flow direction. During this "switch" the tip of the patch pipette and thereby the cytosolic side of the patch were exposed to the filament solution. The rate of solution exchange of each individual patch was determined by measuring the shift of the open channel K^+ current as a result of changes in $[K^+]$ between PSS and the filament solution.

For the studies of Ca^{2+}-dependent activation, the patch was held continuously in the filament solution, and the bath was perfused by one of the test solutions listed in Table I. Different test solutions were applied to the cytosolic side of the patch by switching the filament away from the patch for 200 ms. Most experiments were performed at room temperature (22 ± 2°C). In another series of experiments a temperature-controlled chamber was used to study the influence of changes of temperature between 16 and 37°C.

Single channel currents were recorded with an RK 300 patch amplifier (Biologic, Echirolles, France). A PDP 23 minicomputer (Digital Equipment Corp., Maynard, MA) generated the command signals and controlled the timing of the liquid filament switch. The currents were low pass filtered at 1 kHz, sampled at 50 or 5 kHz, digitized, and stored in records of 2,000 points. 150 data points were sampled before, 1,000 during, and 850 after exposure to the test solution.

TABLE I

Composition of the Test Solutions

KCl	EGTA	HDTA	HEPES	Added $CaCl_2$	Free $[Ca^{2+}]$
mM	*mM*	*mM*	*mM*	μM	μM
150	1	0	10	955	3
150	0	1	10	835	6
150	1	0	10	994	20
150	0	1	10	440	20
150	0	0	10	45	50
150	0	0	10	316	320
150	0	0	10	1,000	1,000

The pH of each solution was adjusted to 7.2 with KOH. Added $CaCl_2$ was calculated according to the program of Fabiato (1988), and the resulting free $[Ca^{2+}]$ was measured and adjusted with a Ca^{2+} electrode system if necessary.

Mean currents were averaged from an adequate number of records (between 10 and 100). In the plots, data points represent the mean ± SE from 4–12 patches. Theoretical curves were fitted with the Levenberg-Marquard nonlinear least-squares algorithm (Brown and Dennis, 1972), and statistical significance was verified by Student's t test ($P < 0.05$).

RESULTS

Speed of Solution Exchange

The speed of the solution change is critical for the intended type of kinetic analysis. It was tested in a first set of experiments studying the effect of K^+ concentration jumps on the open channel current. In PSS containing 5.4 mM K^+, the membrane was clamped to the calculated K^+ equilibrium potential (+80 mV in the whole cell convention). The jump from PSS to the filament solution containing 150 mM KCl, 0.2 mM $CaCl_2$, and 10 mM HEPES (pH 7.2) induced an outward current which decayed upon return to PSS (Fig. 1, *A* and *B*). The time course of the onset of the

outward current was fitted with

$$I(t) = I_{max} \cdot \left(1 - \exp \frac{t_{delon} - t}{\tau_{on}}\right)$$ (1)

for $t \geq t_{delon}$ and the time course of the offset was fitted with

$$I(t) = I_{max} \cdot \exp \left(\frac{t_{deloff} - t}{\tau_{off}}\right)$$ (2)

for $t \geq t_{deloff}$ (see Fig. 1 C). The fits of the mean currents yielded time constants (τ_{on}, τ_{off}) between 0.2 and 1 ms and delay terms (t_{delon}, t_{deloff}) between 1 and 5 ms.
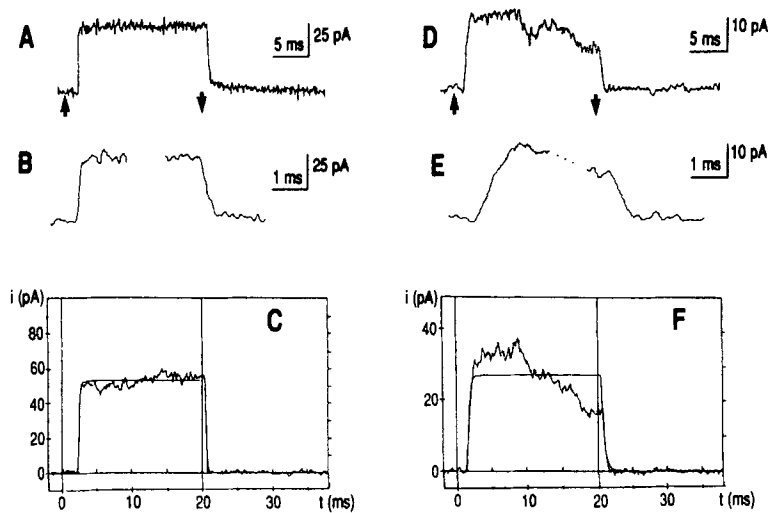

FIGURE 1.   Test of the speed of solution exchange. To an inside-out multi-channel patch, a liquid filament switched the K$^+$ concentration from 5.4 to 150 mM (↑) and back to 5.4 mM (↓) at 0 and 20 ms, respectively. Records A–C are from a different patch than records D–F. Filament solution contained 0.2 mM Ca^{2+} in A–C, but 1 mM EGTA in D–F. Bathing solution was PSS and holding potential was +80 mV. B and E show traces A and D on an expanded time scale. C and F show the mean currents fitted according to Eq. 1 and 2. The time constants τ_{on} and τ_{off} were 0.17 and 0.11 ms in C, and 0.41 and 0.46 ms in F.

Before each Ca^{2+} activation experiment, the speed of the solution change was tested by a 20-ms switch from the PSS (5.4 mM K$^+$, 0.2 mM Ca^{2+}) to the Ca^{2+}-free filament solution (150 mM K$^+$, 1 EGTA) that was used throughout the experiment. Fig. 1, D–F, shows two effects of this switch. The initial rapid rise in outward current is attributed to the change in the K$^+$ driving force. The later and slower decay is attributed to the Ca^{2+} removal that induces the closure (deactivation) of the maxi K$^+$ channels. The parameters of Eqs. 1 and 2 depended on the position of the electrode's tip relative to the border of the liquid filament. This position was adjusted manually for minimizing these parameters. For the studies of Ca^{2+}-dependent activation of maxi K$^+$ channels, only those patches were accepted where t_{delon} and

t_{deloff} were <5 ms and where both time constants (τ_{on} and τ_{off}) were <1 ms. The response to a changed $[K^+]$ was always faster than the response due to a changed $[Ca^{2+}]_i$. For example, the switch from $[Ca^{2+}]_i = 200$ μM to $[Ca^{2+}]_i < 10$ nM (EGTA) reduced the K^+ current at a rate that was slower than the effects of elevated $[K^+]$ by at least one order of magnitude (see Fig. 1, D–F). The difference in time course suggests a different mode of action. It is most likely that the effects of changed $[K^+]$ become steady as soon as the new electrochemical gradient has been established at the tip of the electrode. The $[Ca^{2+}]_i$ response requires additional time due to diffusion from the tip to the inner side of the omega-shaped membrane patch and

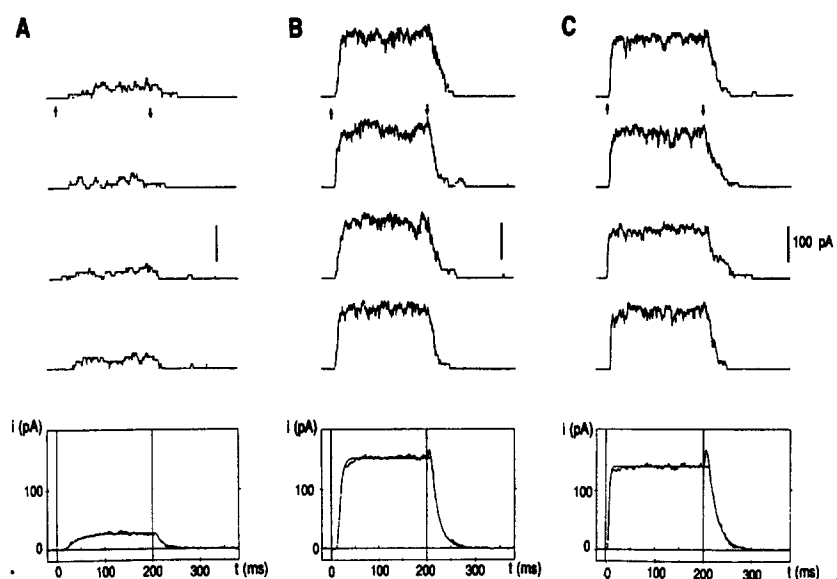FIGURE 2. Ca^{2+}-dependent activation of maxi K^+ channels. All traces were recorded from the same patch. Before the start of the Ca switch ($\uparrow$, 0 ms) $[Ca^{2+}]_i$ was <10 nM. At time zero $[Ca^{2+}]_i$ was switched to 3, (A), 20 (B), and 1,000 μM (C), respectively. After 200 ms ($\downarrow$) $[Ca^{2+}]_i$ was returned to <10 nM. Membrane potential was +30 mV. At the bottom, mean currents of 30 (A) or 10 (B, C) sweeps were fitted according to Eqs. 12 and 13. The fitted activation time constant (τ_a) and deactivation time constant (τ_d) were (A, 3 μM) $\tau_a = 18.7$, $\tau_d = 44.2$ ms; (B, 20 μM) $\tau_a = 5.2$ ms, $\tau_d = 45.6$ ms; and (C, 1,000 μM) $\tau_a = 2.0$ ms, τ_d 47.7 ms, respectively.

due to the reactions following the binding of Ca^{2+} ions to the protein. The different nature may justify the procedure of Eqs. 1 and 2; that is, the subtraction of the delay terms of the filament switch (t_{delon}, t_{deloff}) from the time course of the activation and deactivation of maxi K^+ channels.

Time Course of Ca^{2+}-dependent Activation of Maxi K^+ Channels

Fig. 2 shows five individual current tracings together with the mean currents under the influence of the $[Ca^{2+}]_i$ switch. Before the switch $[Ca^{2+}]_i$ was <10 nM. During the switch $[Ca^{2+}]_i$ rose to 3 μM (Fig. 2 A), 20 μM (Fig. 2 B), and 1,000 μM (Fig. 2 C),

respectively. During the switch the channels started to open after a short delay which was insensitive to the different $[Ca^{2+}]_i$ (see also Fig. 8 A). Activation was complete within 10 (1,000 μM $[Ca^{2+}]_i$) to 100 ms (3 μM $[Ca^{2+}]_i$), and then the currents remained constant; i.e., they did not inactivate during the 200-ms switch. Comparing the switch to 20 μM with the one to 3 μM shows that the time course of activation became faster and the sustained current larger with the higher $[Ca^{2+}]_i$ (cf. Fig. 2 B and Fig. 2 A). The switch to 1,000 μM activated the current with an even faster time course; the sustained current, however, had an amplitude lower than during activation by 20 μM Ca^{2+}.

At the end of the 200-ms switch, during return of $[Ca^{2+}]_i$ to < 10 nM, the current deactivated. The time course of deactivation was independent of the preceding $[Ca^{2+}]_i$ (see also Fig. 9 B). However, the switch from the preceding 20 or 1,000 μM $[Ca^{2+}]_i$ induced an initial transient increase in outward current before deactivation. Both peaks in outward current had the same absolute amplitude; hence, it was more obvious after 1,000 μM than after 20 μM $[Ca^{2+}]_i$. Later in this paper a fast open channel block by high $[Ca^{2+}]_i$ and its removal upon return to < 10 nM $[Ca^{2+}]_i$ will be discussed as an underlying mechanism.

Fig. 3 shows the time course of activation and deactivation for 200-ms switches to 20 μM $[Ca^{2+}]_i$ at patch membrane potentials of -50, -10, and $+50$ mV. Comparison of the mean K^+ currents reveals that more positive potentials accelerate Ca^{2+} activation and decelerate deactivation of maxi K^+ channels (compare -50 mV [panel A] with $+50$ mV [panel C] in Fig. 3). The activation and deactivation time course was studied over a wide range of membrane potentials at six different $[Ca^{2+}]_i$ in > 50 patches. Later in this paper the dependence of the time constants on membrane potential is fitted by a model.

Amplitude of Open Channel Current

The amplitude of the open channel current was evaluated from amplitude histograms to which multiple Gaussian distributions were fitted (Fig. 4). The independence of individual channel openings was tested by binomial distributions fitted to the peaks of the histograms (Barrett, Magleby, and Pallotta, 1982). In addition, the fit yielded the number of individual channels, N, in the patch and the single channel current, i. Once N was known, the steady-state (maximal) open probability, P_o, was determined by

$$P_o = \frac{I_{max}}{N \cdot i} \tag{3}$$

For the actual membrane potential and Ca^{2+} concentration, the single channel current, i, was taken from the mean values of Fig. 5, whereas the I_{max} was the actual steady-state value of the fit through the mean current (e.g., Fig. 3). The well-defined peaks in the amplitude histogram (Fig. 4) did not change to higher i with increasing $[Ca^{2+}]_i$, proving that the enlargement of K^+ current by Ca^{2+} was not due to a change of the single channel conductance. Instead, the increase in mean current could be attributed to a higher open probability, P_o (i.e., to a $[Ca^{2+}]_i$-activated channel gating).

Fig. 5 shows the dependence of open channel current on membrane potential with $[Ca^{2+}]_i$ as parameter. Between -90 and $+10$ mV, all data followed a linear

current–voltage relation with a slope conductance of 274 pS and an intercept of −7.8 mV. At very negative potentials (−110 mV) the conductance was slightly diminished. At positive potentials, Ca^{2+} concentrations of 320 and 1,000 μM reduced the single channel conductance (open channel block) below the values measured at 3, 6, or 20 μM. The curves had a reversal potential of −8 mV, which is attributed to the junction potential; the system was zeroed in PSS before the giga-seal was formed. For purposes of clarity, this junction potential will not be subtracted.
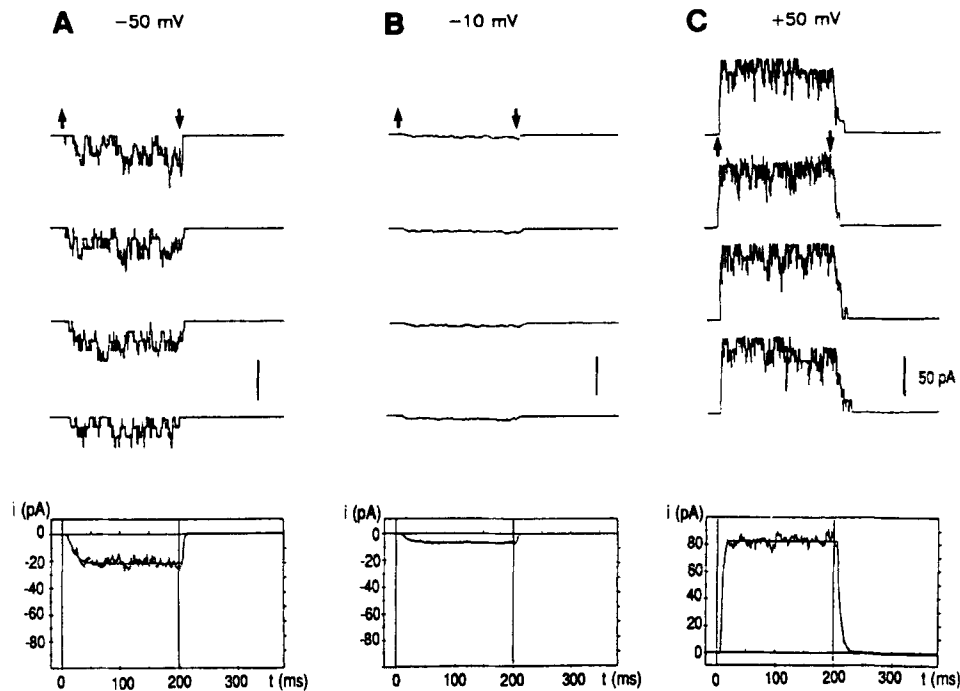

FIGURE 3. Influence of membrane potential on activation of maxi K^+ channels by 20 μM $[Ca^{2+}]_i$. Patch holding potential was −50 mV (*A*), −10 mV (*B*), and +50 mV (*C*), respectively. For further details see Fig. 2. (*Bottom*) Mean currents of 10 tracings each. The fitted activation (τ_a) and deactivation time constants (τ_d) were (*A*, −50 mV) τ_a = 6.4, τ_d = 8.1 ms; (*B* −10 mV) τ_a = 9.5, τ_d = 10.3 ms; and (*C* +50 mV) τ_a = 2.8 ms, τ_d = 18.8 ms, respectively.

Dependence of P_o on $[Ca^{2+}]_i$ and Membrane Potential

Since the Ca^{2+}-activated current did not inactivate during the 200-ms $[Ca^{2+}]_i$ switch, peak P_o and steady-state open probability (P_o) were equal. Fig. 6 shows the plot of steady-state P_o versus pCa = −log ($[Ca^{2+}]_i$) for membrane potentials of −50, −10, and +10 mV. First approximations yielded Hill coefficients between 2 and 3; hence, we postulated that three Ca^{2+} binding sites are involved in the activation of maxi K^+ channels. We postulated that the three Ca^{2+} binding sites were equal and independent. Therefore, we fitted the dependence of P_o on $[Ca^{2+}]_i$ with

$$P_0([Ca^{2+}]_i) = P_{0,max}/(1 + K_D/[Ca^{2+}]_i)^3 \tag{4}$$

(see Fig. 6). In case of cooperative Ca^{2+} binding, P_o would be

$$P_0([Ca^{2+}]_i) = P_{0,max}/\{1 + (K_D/[Ca^{2+}]_i)^3\} \qquad (4a)$$

(see Adam, Läuger, and Stark, 1988). P_o was always <1.0; a maximal open probability $P_{o,max}$ of 0.8 ± 0.02 (at all $[Ca^{2+}]_i$'s) was obtained which was utilized for all
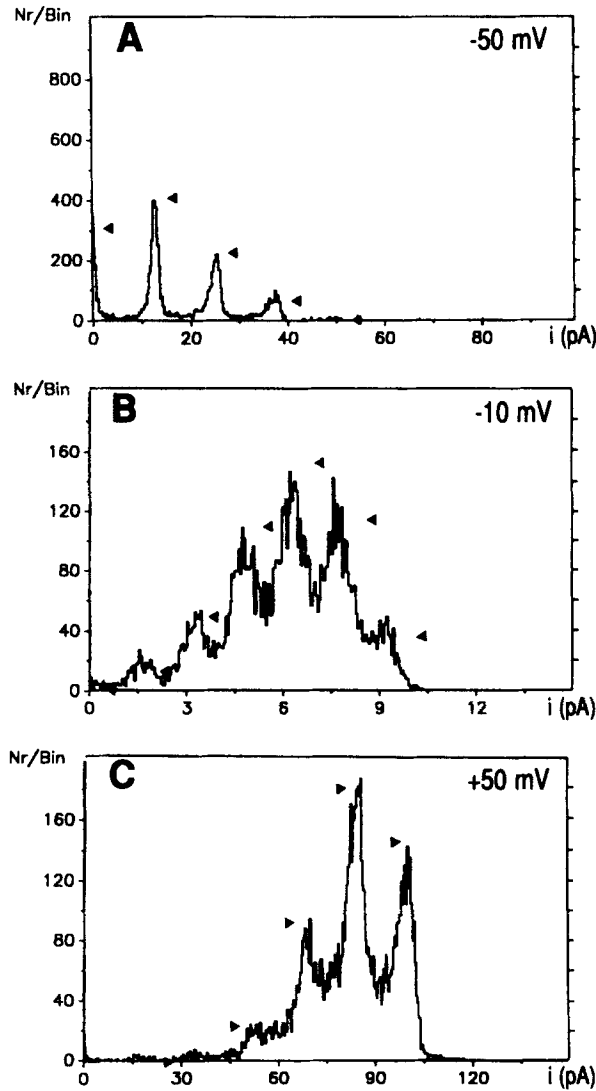

FIGURE 4. Amplitude histograms for the patch shown in Fig. 3. Data points for each histogram are from the corresponding 10 traces used for calculation of mean currents in Fig. 3. Gaussian fit (not shown) and binomial approximation of the histogram peaks (arrowheads) revealed six channels in the patch. Amplitude of single channel current, i, and channel open probability, P_o, were (A -50 mV) -13.0 pA and 0.18; (B -10 mV) 1.6 pA and 0.65; and (C $+50$ mV) 16.8 pA and 0.81, respectively.

subsequent calculations (see Figs. 6 and 7). The apparent dissociation constant K_D decreased with more positive potentials (see inset of Fig. 6). This voltage dependence suggests that the Ca^{2+} binding sites are localized within the electrical field of the membrane (Woodhull, 1973). Hence, the voltage dependence of K_D was fitted by

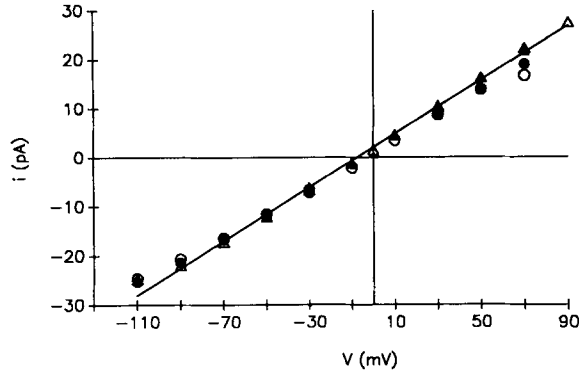$$K_D(V) = K_D(0)\cdot exp[-\delta\cdot V\cdot(z\cdot F/R\cdot T)] \qquad (5)$$

FIGURE 5. Voltage dependence of currents through single Ca²⁺-activated maxi K⁺ channels. The linear fit revealed a slope conductance of 274 pS and a reversal potential of −7.8 mV. Each point represents mean values of 3–15 patches at a Ca²⁺ concentration of 3 μM (*filled triangles*), 20 μM (*empty triangles*), 320 μM (*filled circles*), and 1,000 μM (*circles*). The data at 6 and 50 μM [Ca²⁺]ᵢ (not shown) are not significantly different from the data at 3 and 20 μM.

where V, z, F, R, and T are the membrane potential, the equivalence charge (2), the Faraday constant, the gas constant, and the absolute temperature (251 K), respectively. For 22°C, the term $(z \cdot F / R \cdot T)$ had a value of 12.7 mV. For $V = 0$ mV, the apparent dissociation constant was estimated at $K_D(0) = 2.3$ μM. The Ca²⁺ binding was determined to occur inside the electrical field at an electrical distance $\delta = 0.29$ from the inner side the membrane. By substitution of Eq. 5 into Eq. 4, one obtains the general form that describes both Ca²⁺ and voltage dependence of the open probability:

$$P_0([\text{Ca}^{2+}]_i, V) = 0.8 \cdot \{1 + (K_D(0)/[\text{Ca}^{2+}]_i) \cdot \exp(2 \cdot \delta \cdot V \cdot F / R \cdot T)\}^{-3} \qquad (6)$$
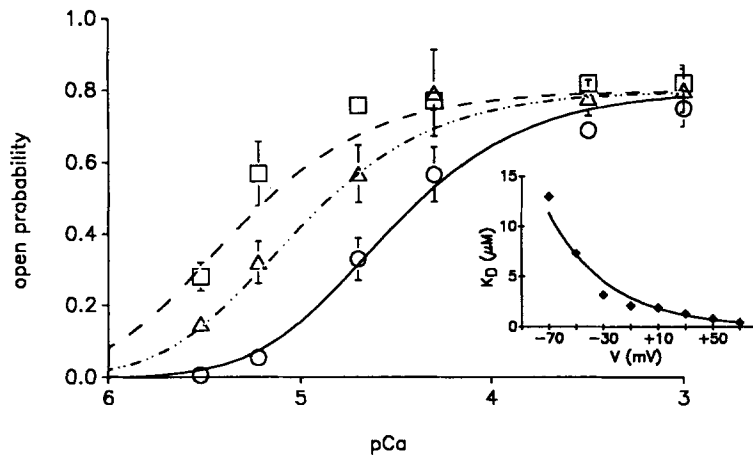

FIGURE 6. Dependence of the open probability of maxi K⁺ channels on [Ca²⁺]ᵢ at steady state (200 ms). Data were measured at a membrane potential of −50 mV (*circles*), −10 mV (*triangles*), or +50 mV (*squares*) and were fitted according to Eq. 4. The inset shows the voltage dependence of the apparent K_D fitted according to Eq. 5.
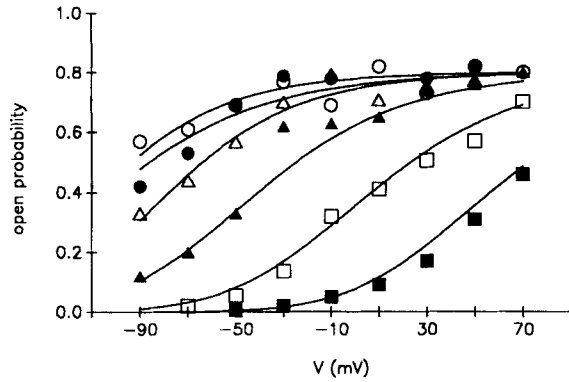
FIGURE 7. Dependence of the open probability of maxi K⁺ channels at steady state on membrane potential with a $[Ca^{2+}]_i$ of 3 μM (*filled squares*), 6 μM (*open squares*), 20 μM (*filled triangles*), 50 μM (*open triangles*), 320 μM (*filled circles*), or 1,000 μM (*open circles*). Data were fitted according to Eq. 6. The evaluated parameters are listed in Table II A.

Eq. 6 can fit the experimental data reasonably well for $[Ca^{2+}]_i \leq 50$ μM (see Fig. 7). From the fit with Eq. 6 the parameters $K_D(0)$ and δ were evaluated. The results show that $[Ca^{2+}]_i$ has no systematic influences on them (see Table II A).

Eq. 6 is based on the assumption (Eq. 4) that the three Ca^{2+} binding sites are independent. This assumption is necessary for the consistency of the model. For comparison, modeling with cooperativity (Eq. 4a) was tried. In such a case, the fit of Eq. 6 to the data of Fig. 6 yielded δ values of ~0.1 A Ca^{2+} binding at δ = 0.1,

TABLE II

Parameters for the Description of $P_o(V,[Ca^{2+}]_i)$

(A) Evaluation of steady-state data. The apparent dissociation constant for Ca^{2+} at 0 mV $K_D(0)$ and the electrical distance of the Ca^{2+} binding sites from the cytoplasmic side of the membrane δ were deter-mined by fit of Eq. 6 to the experimental data shown in Fig. 7. From these K_D and δ the value α(0) was derived from α(0) = $K_D/β$ and $δ_α = δ - δ_β$ using β(0) = 27 s⁻¹ and $δ_β$ = 0.15.

$[Ca^{2+}]_i$	$K_D(0)$	δ	α(0)	$δ_α$
μM	μM		μM⁻¹s⁻¹	
3	3.7	0.23	7.3	0.08
6	1.9	0.33	14.2	0.18
20	1.7	0.34	15.9	0.19
50	1.2	0.39	22.5	0.24
320	5.7	0.33	4.7	0.18
1,000	8.5	0.41	3.2	0.26

(B) Activation parameters from kinetic analysis. α(0) was estimated from the activation time constant $τ_α$ according to Eq. 17. $δ_α$ was obtained by approximation of the voltage dependence α(V) to Eq. 8.

$[Ca^{2+}]_i$	α(0)	$δ_α$
μM	μM⁻¹s⁻¹	
3	6.6	0.21
6	5.0	0.14
20	5.3	0.14
50	1.5	0.10
320	0.5	0.15
1,000	0.4	0.17

however, predicts a voltage dependence that is incompatible with the observed steady-state data (Figs. 6 and 7) and the time constants of activation and deactivation (Fig. 9 and Eq. 10; see below).

A Kinetic Model of $I_{K(Ca)}$

$$R + Ca^{2+} \underset{\beta}{\overset{\alpha}{\rightleftharpoons}} RCa^{2+} \tag{7}$$

describes Ca^{2+} binding to a site R with association and dissociation rate constants α and β, respectively. According to Villarroel, Alvarez, Oberhauser, and Latorre (1988), the voltage dependence of α and β is given by:

$$\alpha(V) = \alpha(0) \cdot \exp{(2\delta_\alpha \cdot V \cdot F/R \cdot T)} \tag{8}$$

and

$$\beta(V) = \beta(0) \cdot \exp{(-2\delta_\beta \cdot V \cdot F/R \cdot T)} \tag{9}$$

with

$$\delta = \delta_\alpha + \delta_\beta \tag{10}$$

and

$$K_D = \beta/\alpha \tag{11}$$

The strong influence of $[Ca^{2+}]_i$ on the activation time course (Fig. 2) implies that it is the binding of Ca^{2+} that is the rate-limiting state in the activation. Eq. 6 postulates that the voltage dependence of P_o resides mostly in the Ca^{2+}-binding steps. Eq. 6 predicts that for $[Ca^{2+}]_i \gg K_D$ the influence of positive membrane potential on P_o becomes insignificant. The results of Figs. 6 and 7 support this prediction for $[Ca^{2+}]_i \geq 50$ μM and positive potentials (low K_D). According to Eq. 4, we describe the time course of the activation of the K^+ current by a cubic power function:

$$I_{K(Ca)}(t) = N \cdot i \cdot n^3 \cdot 0.8 \tag{12}$$

with

$$n = n(t) = n_\infty - (n_\infty - n_0) \cdot \exp{[-(t - t_{del})/\tau]} \tag{13}$$

for $t \geq t_{del}$. In the steady state n approaches n_∞, which is given by

$$n_\infty = \frac{\alpha \cdot [Ca^{2+}]_i}{\alpha \cdot [Ca^{2+}]_i + \beta} \tag{14}$$

whereas the time constant τ is defined by

$$\tau = \frac{1}{\alpha \cdot [Ca^{2+}]_i + \beta} \tag{15}$$

Eqs. 12–15 coincide with the scheme proposed by Hodgkin and Huxley (1952). Although $n(t)$ rises exponentially from zero, the cubic term contains mixed contributions; that is, n^3 rises along an S-shaped curve, imitating the sigmoidity in the Ca^{2+}

activation. During deactivation, n relaxes toward $n_\infty = 0$; that is, Eq. 13 simplifies to $n(t) = n_0 \cdot \exp\{-(t - t_{del})/\tau\}$ and the cubic function of $[n(t)]^3$ falls exponentially.

As a result of the maximal open probability being 0.8, non–rate-limiting steps a and b had to be introduced into the calculation (a/(a + b) = 0.8). Then, the following reaction scheme for the Ca^{2+}-activated K^+ channel was obtained:
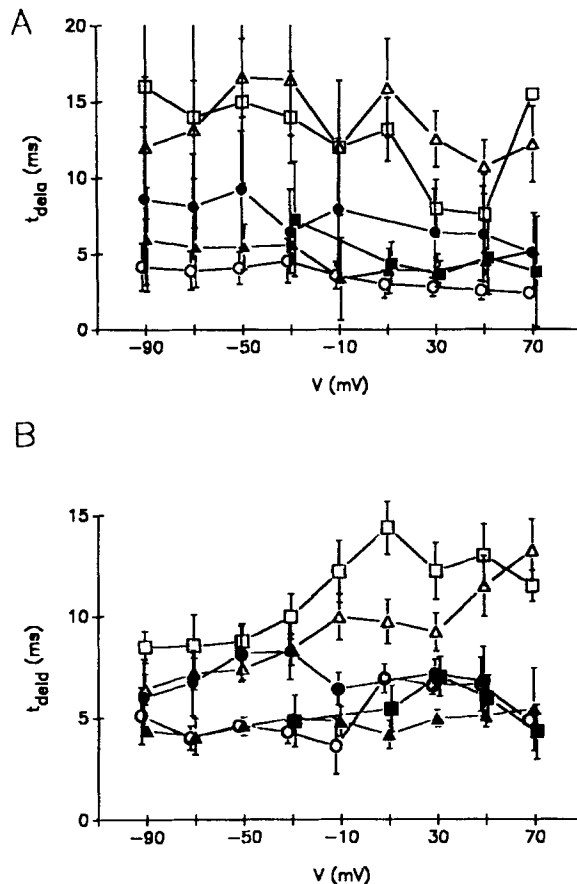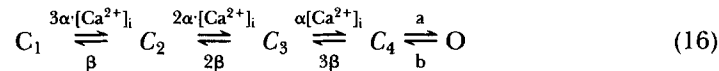
$$C_1 \underset{\beta}{\overset{3\alpha \cdot [Ca^{2+}]_i}{\rightleftharpoons}} C_2 \underset{2\beta}{\overset{2\alpha \cdot [Ca^{2+}]_i}{\rightleftharpoons}} C_3 \underset{3\beta}{\overset{\alpha[Ca^{2+}]_i}{\rightleftharpoons}} C_4 \underset{b}{\overset{a}{\rightleftharpoons}} O \tag{16}$$

FIGURE 8. The delay preceding channel activation (A: t_{dela}) and channel deactivation (B: t_{deld}) as a function of membrane potential with a $[Ca^{2+}]_i$ of 3 μM (filled squares), 6 μM (open squares), 20 μM (filled triangles), 50 μM (open triangles), 320 μM (filled circles), or 1,000 μM (open circles).

The hypothesis that three Ca^{2+}-binding sites are involved in the activation of $I_{K(Ca)}$ is based on three arguments. First, the dependence of steady-state P_0 on $[Ca^{2+}]_i$ yielded Hill coefficients of 2–3. Second, the activation time course of $I_{K(Ca)}$ was modeled best (Horn, 1987) when a Hodgkin-Huxley exponent of 3 was used in Eq. 12. Finally, Eq. 15 shows that the activation time constants $\tau_a = \{\beta + \alpha \cdot [Ca^{2+}]_i\}^{-1}$ must always be smaller than the deactivation time constants $\tau_d = \beta^{-1}$ (Eq. 15 with $[Ca^{2+}]_i = 0$). With the constraint $\tau_a < \tau_d$, fits of Eqs. 12 and 15 to the experimental data were possible only if the exponent in Eq. 12 was ≥ 3.

The rate constants α and β were evaluated by fitting Eq. 12 to the activation and deactivation time course of the mean currents (bottom panels in Figs. 2 and 3). For this fit, there was a problem with the delay between the jump in Ca^{2+} concentration and the change in mean current (already demonstrated in Figs. 2 and 3). The delay before activation (t_{dela}) was not significantly different from the delay before deactivation (t_{deld}). The data are scattered between 2 and 20 ms and a clear dependence on voltage or $[Ca^{2+}]_i$ was not indicated (Fig. 8). t_{dela} and t_{deld} were several times longer than the delay terms t_{delon} and t_{deloff}, evaluated from jumps in $[K^+]$; hence, the
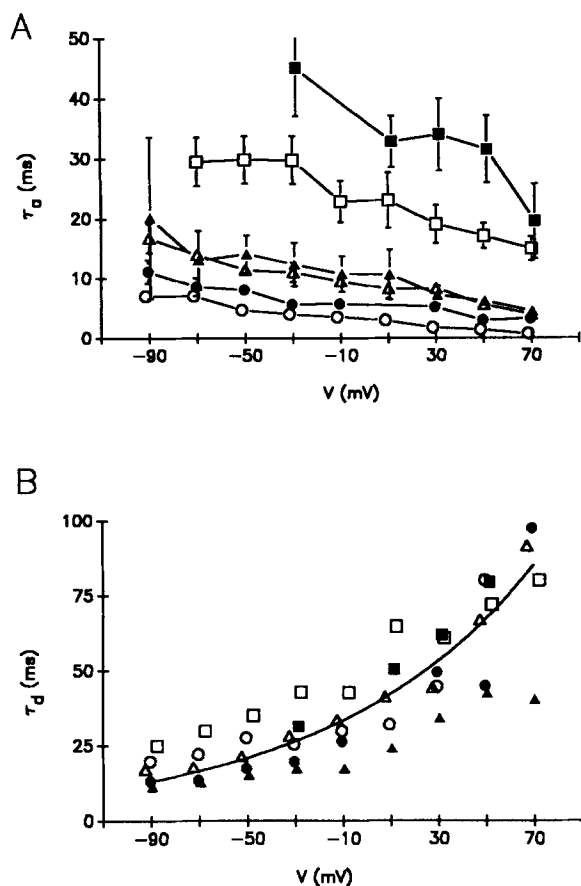

FIGURE 9. Influence of membrane potential and $[Ca^{2+}]_i$ on (*A*) time constants of activation (τ_a) and (*B*) time constants of deactivation (τ_d). $[Ca^{2+}]_i$ was 3 μM (*filled squares*), 6 μM (*open squares*), 20 μM (*filled triangles*), 50 μM (*open triangles*), 320 μM (*filled circles*), or 1,000 μM (*open circles*). Data were evaluated by approximation of mean currents by Eqs. 11 and 12. (*B*) For the fit of $\tau_d(V)$ according to Eqs. 14 and 9 τ_d values from experiments with different $[Ca^{2+}]_i$ were lumped together, yielding $\beta(0) = 27$ s^{-1} and $\delta_\beta = 0.15$.

subtraction of the time of the K^+ concentration change only incompletely corrected for the delay measured during Ca^{2+} concentration jumps. Below we will discuss differences in the diffusional access of K^+ and Ca^{2+} from the electrode's tip of the maxi K^+ channel in the membrane of the inside-out patch.

Eq. 15 predicted that the deactivation time constant τ_d is independent of $[Ca^{2+}]_i$. The results supported this prediction. When the deactivation time constants τ_d were correlated with $-\log([Ca^{2+}]_i)$ the correlation coefficient was 0.08, which is not significantly different from zero. Fig. 9 *B* shows the voltage dependence of τ_d for

different $[Ca^{2+}]_i$ as a parameter; again the influence of $[Ca^{2+}]_i$ is not significant. Hence, all ß values for 0 mV membrane potential and different $[Ca^{2+}]_i$ were pooled and Eqs. 9 and 15 were fitted, and this fit yielded 27 s^{-1} for $\beta(0)$ and 0.15 for δ_β.

The activation time constants, τ_α, clearly depended on both voltage and $[Ca^{2+}]_i$ (see Fig. 9A). From $\tau_\alpha(V, [Ca^{2+}]_i)$, using Eqs. 3, 12, 14, and 15, the corresponding rate constants $\alpha(V)$ were calculated by

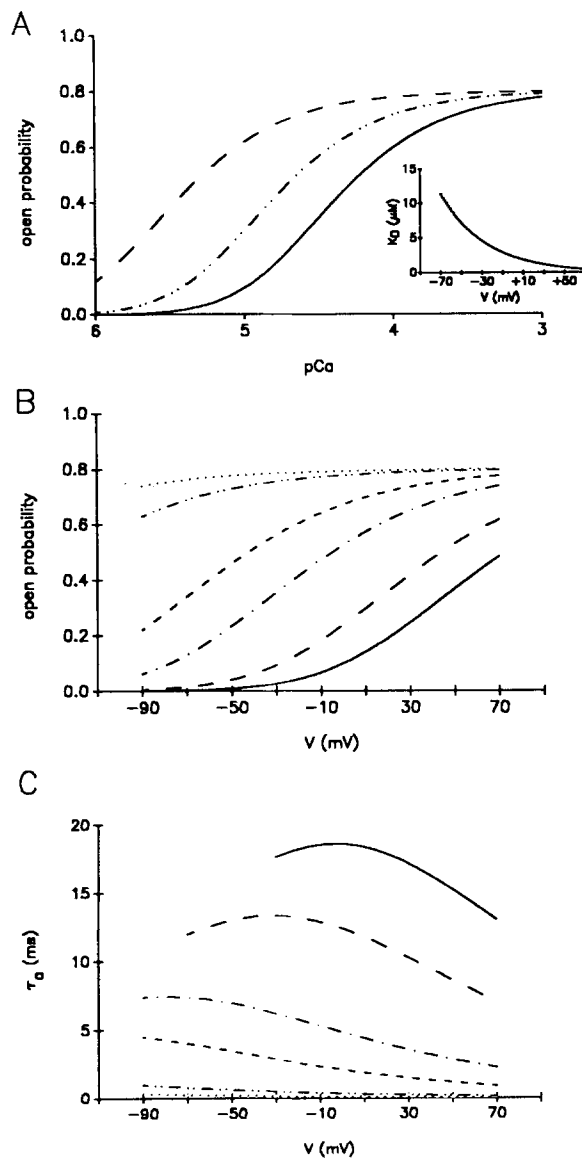$$\alpha(V) = \sqrt[3]{\frac{(P_0/0.8)}{\tau_a \cdot [Ca^{2+}]_i}} \qquad (17)$$

FIGURE 10. Predictions of a model for Ca^{2+}-dependent activation of maxi K^+ channels with three noncooperative voltage-dependent Ca^{2+} binding sites. (A) Dependence of open probability on $[Ca^{2+}]_i$ at different membrane potentials (solid line, -50 mV; dot-dashed line, -10 mV; dashed line, $+50$ mV). (Inset) Voltage dependence of the apparent K_D. See Fig. 6 for comparison. (B) Dependence of open probability on membrane potential at various levels of $[Ca^{2+}]_i$. See Fig. 7 for comparison. (C) Dependence of the activation time constant τ_a on membrane potential at different levels of $[Ca^{2+}]_i$. See Fig. 9A for comparison. In B and C, different $[Ca^{2+}]_i$ is marked by the line pattern: solid (3 µM), dashed (6 µM), dot-dashed (20 µM), short-dashed (50 µM), dot-dot-dashed (320 µM), and dotted (1,000 µM).

The fit of with Eq. 8 to $\alpha(V)$ yielded $\alpha(0)$ and δ_α for each used Ca^{2+} concentration; the results are given in Table II B with $[Ca^{2+}]_i$ as parameter.

Table II A compares the parameters $\alpha(0)$ and δ_α that were evaluated from steady-state data with those evaluated from the activation time course (Table II B). According to the fit of $K_D(V)$ using Eq. 5 and the values listed in Table II, we estimated that $K_D(0) = 3$ μM, $\delta = 0.31$, $\alpha(0) = 9$ $\mu M^{-1}s^{-1}$, and $\delta_\alpha = 0.16$, respectively. Systematic differences were found for $[Ca^{2+}]_i > 20$ μM where the $\alpha(0$ mV)'s from kinetic analysis (Table II B) were distinctly lower than their counterparts from steady state. Apart from this discrepancy, the model adequately predicts the influence of $[Ca^{2+}]_i$ and voltage on open probability, P_o, activation, and deactivation. The predictions are summarized in Fig. 10. Although the predicted voltage depen-
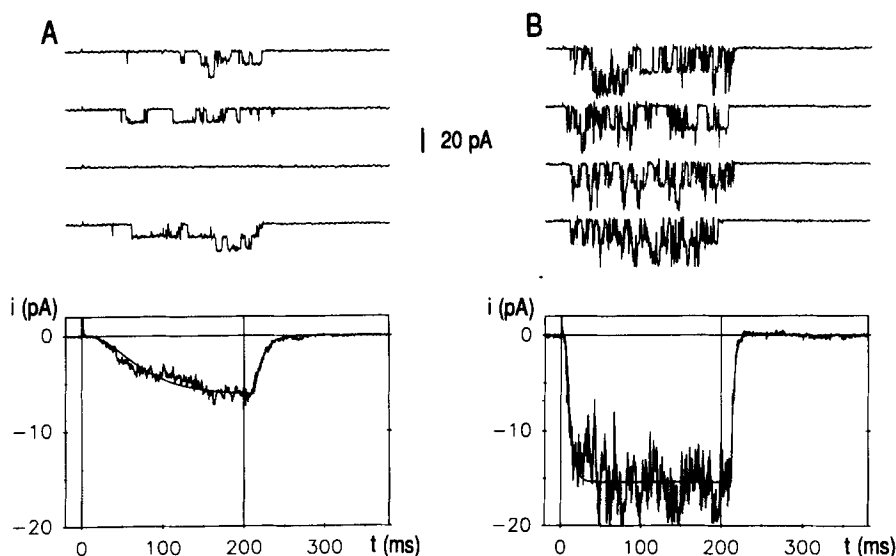

FIGURE 11. Influence of temperature on activation and deactivation of maxi K+ channels. Activating Ca^{2+} concentration, 200 μM; patch membrane potential, -50 mV. Bath temperature, 16°C (A) and 37°C (B). For further details see Fig. 2. The time constants of activation (τ_a) and deactivation (τ_d) were (A: 16°C) $\tau_a = 35.5$ ms, $\tau_d = 42.1$ ms and (B: 37°C) $\tau_a = 5.5$ ms, $\tau_d = 8.3$ ms, respectively.

dence of the activation time constants τ_α (Fig. 10 C) can be compared with the voltage dependence of the τ_α from kinetic analysis (see Fig. 9 A for 3, 6, and 20 μM $[Ca^{2+}]_i$), there is a wide range of experimental error. The variability in temperature by approximately $\pm 2°C$ could be a reason.

Free Energy of Ca^{2+} Binding and Ca^{2+} Dissociation

The free energy of Ca^{2+} binding and Ca^{2+} dissociation determines the time course of both activation and inactivation of maxi K+ channels. For the binding energy (ΔG) at 0 mV, -7.5 kcal·mol^{-1} was estimated from a $K_D(0$ mV) of 3 μM. Dissociation of Ca^{2+} from the binding site requires the unbinding energy, $\Delta G'$, which can be calculated

from the rate constant of deactivation $\beta(0)$ by

$$\beta(0) = k \cdot T/h \cdot \exp(\Delta G'/RT) \tag{18}$$

where h is the Planck constant and $k \cdot T/h$ is the molecular vibration period (Hille, 1984). For $\beta(0\ \text{mV}) = 27\ \text{s}^{-1}$, a value of 15.3 kcal·mol^{-1} was calculated for $\Delta G'$. To dissociate from their binding sites, the Ca^{2+} ions must overcome this energy barrier.

Independent of Eq. 18, the free energy for Ca^{2+} dissociation from the binding site can be evaluated from the temperature dependence of β. With an additional set of experiments, $\beta(V, T)$ was measured at five different temperatures using concentra-
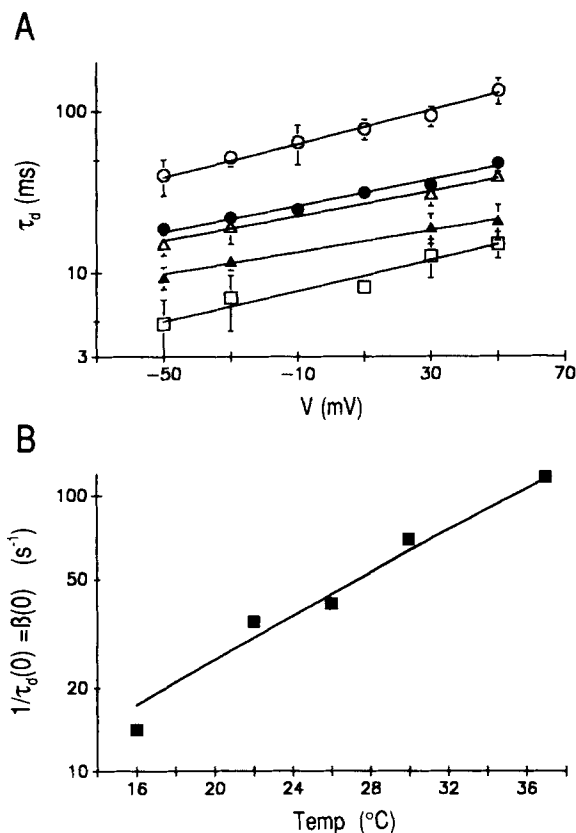
A

B

FIGURE 12. Temperature dependence of deactivation of $I_{K(Ca)}$. Different temperatures are marked by symbols (open circles, 16°C; filled circles, 22°C; open triangles, 26°C; filled triangles, 30°C; open squares, 37°C). The deactivation time constants were evaluated using Eqs. 11 and 12. The straight lines are the approximations according to Eq. (9). For the free energy of Ca^{2+} dissociation, a $\Delta G' = 16$ kcal/mol was evaluated from the fit of the $\beta(0) = \tau_d(0)^{-1}$-values, depicted in B, with $\beta(0, T) = \exp(C - \Delta G'/RT)$, where C is an arbitrary constant.

tion jumps to 200 μM [Ca^{2+}]$_i$. The mean currents of Fig. 11 indicate that an increase in the bath temperature from 16 to 37°C accelerated the time course of both deactivation and activation (see legend to Fig. 12). The voltage dependence of the deactivation time constant τ_d with temperature T as a parameter is shown in Fig. 12 A. The temperature does not obviously change the voltage dependence of τ_d as verified by the δ_β listed in Table III. Fig. 12 B shows the temperature dependence of $1/\tau_d = \beta(0, T)$. From this temperature dependence the free energy for Ca^{2+} ion dissociation is estimated to be $\Delta G^* = 16$ kcal/mol, which is close to the above calculated $\Delta G'$ of 15.3 kcal·mol^{-1}. The results measured at different temperatures

also provide information on some of the experimental variability. Assuming that the uncontrolled room temperature would have fluctuated from 20 to 24°C, this would have increased ß from 25 to 38 s⁻¹ (Fig. 12) and reduced τ_d = 1/ß from 40 to 26 ms. Hence, temperature fluctuations can easily account for the variability of τ_d illustrated in Fig. 9.

Consistency with Single Channel Recordings

The test of the validity of our model on the single channel level was hampered because the channels were found in clusters; only 1 of ~100 patches contained a single channel. From all openings and closures during the increased $[Ca^{2+}]_i$ a mean closed and a mean open time, as well as the waiting time to the first opening, were evaluated. Because of the limited number of events, the data were insufficient for the conventional histograms and fits by multi-exponential equations; as customary for single channel events, therefore, they were plotted as a function of P_o. P_o was evaluated during jumps of $[Ca^{2+}]_i$ to 6 or 50 μM and at membrane potentials clamped to values between −70 and +50 mV. For an increase in P_o from 0.05 to 0.7

TABLE III

Temperature Dependence of Deactivation of $I_{K(ca)}$

T	β(0)	δ_β
°C	s^{-1}	
16	14.1	0.15
22	35.0	0.12
26	40.7	0.11
30	69.0	0.10
37	106.4	0.15

Values were calculated from Eqs. 9 and 15.

the mean closed time decreased by a factor of five. Simultaneously, there was a fivefold increase in the waiting time to the first opening after the rapid increase in $[Ca^{2+}]_i$ (first latency). This behavior is predicted by the model (Eq. 16) which attributes the rise of P_o to the increase in the association rate constant α. However, other models involving a Ca^{2+}-binding step leading to channel isomerization could explain the behavior as well. There was also a slight enlargement of the averaged open time, confirming earlier reports (Methfessel and Boheim, 1982; Magleby and Pallotta, 1983*a*; Moczydlowski and Latorre, 1983), with the interpretation that a decrease in shut times causes an increased underestimation of closings and thereby an artificial rise in open times (Moczydlowski and Latorre, 1983). In conclusion, the limited single channel data are consistent with the proposed model for gating of the Ca^{2+}-activated maxi K^+ channels.

DISCUSSION

The channels of this study belonged to the class of "BK" or "maxi" K^+ channels because their conductance was 274 pS in symmetrical K^+ solution. From the same

inside-out patches we could record the currents without significant changes of the gating for 1 h or longer. Due to their high conductance and their stability, maxi K^+ channels have been analyzed in a variety of preparations (for a recent review, see Latorre, Oberhauser, Labarca, and Alvarez, 1989). In the literature, the dependence of $I_{K(Ca)}$ on Ca^{2+} and on the voltage has been well described for the steady state, and the results have led to gating schemes containing more than five closed and up to four open states (Magleby and Palotta, 1983a, b; McManus and Magleby, 1988). However, general agreement is missing with regard to two questions (see Latorre et al., 1984, 1989): (a) which of the steps in the gating scheme are rate limiting? and (b) Does the voltage dependence reside in the Ca^{2+} binding or in the following change of channel conformation? The questions may be answered by experiments analyzing the maxi K^+ channels during rapid changes in $[Ca^{2+}]_i$. Here we analyzed the effect of "jumps" in $[Ca^{2+}]_i$ on the mean currents through macro-patches and obtained information on the kinetics of Ca^{2+}-mediated activation and deactivation of maxi K^+ channels. This information is complementary to that obtained from steady-state single channel analysis.

Block of Single Channel Current

At strong positive or negative potentials, the open channel conductance was reduced, probably due to a fast open channel block by divalent cations. The block could not be resolved by the present recording system. A fast flickering block of K^+ inward current by extracellular Mg^{2+} has been reported by Christensen and Zeuthen (1987), and the block of K^+ outward current by intracellular Ca^{2+} has been reported by Eisenman, Latorre, and Miller (1986). The open channel block by $[Ca^{2+}]_i$ may be responsible for the reduction of the maximal outward current observed during the jumps of $[Ca^{2+}]_i$ to 20 or 1,000 μM, respectively (Fig. 2, B and C). Relief of the block on wash-out of $[Ca^{2+}]_i$ may be responsible for the initial hump in outward current during the return from 1,000 or 20 μM $[Ca^{2+}]_i$ to <10 nM (see Fig. 2 C). Our results indicate that the relief of open channel block is faster than the Ca^{2+}-dependent deactivation (Fig. 2 C); however, this comparison was not analyzed in detail.

The Delay Term

Upon a rapid jump in $[Ca^{2+}]_i$ the mean currents did not change instantaneously but with a delay. Part of this delay could be attributed to the rate of solution exchange as indicated by the effects of K^+ concentration jumps (terms t_{delon} and t_{deloff}); this part was subtracted (see above). A part of the delay remained (t_{del} in Eq. 13, t_{dela} and t_{deld} in Fig. 8). With the present method of the liquid filament switch, the delay was between 5 and 15 ms, which is about one order of magnitude shorter than the 100-ms delay measured with the concentration clamp method (Brett, Dilger, Adams, and Lancaster, 1986; Ikemoto, Ono, Yoshida, and Akaike, 1989). The dependence of the delays on membrane potential and $[Ca^{2+}]_i$ was not statistically significant (Fig. 8). The delay may be attributed to $[Ca^{2+}]_i$-independent steps in Eq. 16. However, the delay could also arise from the limited rate of the change in Ca^{2+} concentration at the patch of membrane; inside-out patches have been shown to invaginate the tip of the electrode for ≥50 μM (Ruknudin, Song, and Sachs, 1991). Since the space inside the electrode's tip is essentially unstirred, access to the cytosolic side of the

membrane may be limited by the rate of diffusion, provided that the solution exchange at the tip is fast. This property of inside-out patches sets some limitations for the application of the liquid filament method.

In this study patches were accepted only if the preceding test of the solution exchange for K^+ ions completed with delay terms, t_{delon}, of <2 ms. Usually a t_{delon} of ≥ 10 ms went together with a t_{del} of 50 ms or longer. Thus, the delay terms t_{delon} upon $[K^+]$ jumps and t_{del} upon $[Ca^{2+}]_i$ jumps seem to be related, although their absolute values differ. At first, the diffusion coefficient for Ca^{2+} in aqueous solutions was half of that for K^+ (see Hille, 1984). Also, with EGTA buffering the change in Ca^{2+} concentration will be slower than that in K^+ because the new Ca^{2+} solution has to saturate any of the buffer that is left. The results obtained with EGTA (<10 nM or 3 μM $[Ca^{2+}]_i$), HDTA (6 and 20 μM $[Ca^{2+}]_i$), or in the absence of buffers ($[Ca^{2+}]_i > 20$ μM) did not show systematic variations in the delay; hence, this influence might be small. Ca^{2+} ions probably diffuse with binding to residual cytosolic proteins; hence, they may be "seen" by the Ca^{2+} binding sites later than indicated by the effects of the $[K^+]_i$ jumps. Diffusion of Ca^{2+} was a severe problem when the activation time course was very fast (e.g., during the activation of $I_{K(Ca)}$ by 50, 320, and 1,000 μM $[Ca^{2+}]_i$, when the experimental time constants τ_α [Fig. 9 A] were systematically above the predicted ones [Fig. 10 C]).

The Model

The model postulated that the activation of the maxi K^+ channels results from the noncooperative binding of three Ca^{2+} ions. Binding of more than one Ca^{2+} ion has been deduced from the slope of Hill plots (for review, see Latorre et al., 1989; Haylett and Jenkinson, 1990); however, there is some uncertainty because the Hill coefficients are sensitive to such experimental parameters as $[Mg^{2+}]_i$ (Golowasch, Kirkwood, and Miller 1986) or temperature (Grygorczyk, 1987). In this study, the assumption of binding of three Ca^{2+} ions was based on two additional arguments: (a) Binding of three Ca^{2+} ions was required for the best description of the S-shaped activation time course of $I_{K(Ca)}$ (Eq. 12). (b) Binding of three or more Ca^{2+} ions was required to explain the result (Fig. 3) that deactivation could be faster than activation despite the constraint that the deactivation time constants ($\tau_d = \beta^{-1}$) always had to be larger than activation time constants ($\tau_a = (\beta + \alpha \cdot [Ca^{2+}])^{-1}$).

The idea that the voltage dependence resides in the binding of Ca^{2+} ions was introduced by Moczydlowski and Latorre (1983). In the present model, this idea required that the membrane potential had a stronger influence on the apparent K_D (Fig. 6, *inset*) than on the individual association and dissociation constants α and β (see Eqs. 5 and 8–10). As already pointed out, this requirement could be fulfilled only if the Ca^{2+} binding to the three sites was assumed to be noncooperative. With these restrictions, the model yielded a $K_D(0)$ of 3 μM and a δ of 0.31, values that are within the range of the K_D and δ values reported for other preparations (Latorre et al., 1989, Marty 1989). In addition, this study yielded the rate constants of Ca^{2+} binding: the association constant, $\alpha(0$ mV), was 9 $\mu M^{-1}s^{-1}$ and the dissociation constant, $\beta(0$ mV), was 27 s^{-1}. These values are similar to the rate constants $\alpha = 20.5$ $\mu M^{-1}s^{-1}$ and $\beta = 25$ s^{-1} reported for the Ca^{2+}-dependent activation of apamin-sensitive K^+ channels (Gurney, Tsien, and Lester, 1987), despite the fact that these channels have

different biophysical properties and that steps of $[Ca^{2+}]_i$ were generated by a different technique (release of Ca^{2+} from caged compounds).

The model predicted Ca^{2+}-dependent shifts in the dwell time distributions which are consistent with the literature. For example, the model attributes the increase in P_o mostly to the increase in α, which is equivalent to a reduction of the mean closed time (Methfessel and Boheim, 1982; Magleby and Pallotta, 1983a; Moczydlowski and Latorre, 1983) and could be confirmed by our own preliminary single channel data. The model also predicts that the increases in P_o and α should accompany shorter times to the first opening, and this prediction was proven experimentally (see above). Unfortunately, the difficulty of getting patches with single channels hampered further analysis.

The model could account quantitatively for the Ca^{2+}-dependent activation of the maxi K^+ channel when $[Ca^{2+}]_i$ was varied between 2 and 20 μM; however, for $[Ca^{2+}]_i$ > 20 μM, systematic differences between measured and modeled data were found. The differences could suggest that other additional steps become rate limiting when the Ca^{2+} concentrations are high, as indicated by the fast open channel block. However, with the limitations of the present method we cannot exclude the possibility that the channel activation at high $[Ca^{2+}]_i$ was retarded by the limited speed by which Ca^{2+} exchanged at the inner side of the membrane.

The results of this paper clearly demonstrate that changes in intracellular Ca^{2+} concentration can activate maxi K^+ channels within a millisecond time scale. In contrast to Ikemoto et al. (1989), we conclude that the time course is sufficient for the Ca^{2+}-mediated activation of maxi K^+ channels during the 20-ms action potential of the smooth muscle cell. Hence, Ca^{2+} activation of outward currents can contribute to the action potential repolarization, at least in these cells. This idea is supported by the prolongation of the action potential resulting from the pharmacological block of $I_{K(Ca)}$ with low TEA concentrations (Klöckner and Isenberg, 1985).

REFERENCES

Adam, G., P. Läuger, and G. Stark. 1988. Physikalische Chemie und Biophysik. 2nd ed. Springer Verlag, Berlin, Heidelberg, New York, London, Paris, Tokyo. 443.

Barrett, J. N., K. L. Magleby, and B. S. Pallotta. 1982. Properties of single calcium-activated potassium channels in cultured rat muscle. *Journal of Physiology.* 331:211–230.

Brett, R. S., J. P. Dilger, P. R. Adams, and B. Lancaster. 1986. A method for the rapid exchange of solutions bathing excised membrane patches. *Biophysical Journal.* 50:987–992.

Brown, K. M., and J. E. Dennis, Jr. 1972. Derivative free analogues of the Levenberg-Marquard and Gauss algorithms for nonlinear least square approximation. *Numerische Mathematik.* 18:289–297.

Christensen, O., and T. Zeuthen. 1987. Maxi K^+ channels in leaky epithelia are regulated by intracellular Ca^{2+}, pH and membrane potential. *Pflügers Archiv* 408:249–259.

Eisenman, G., R. Latorre, and C. Miller. 1986. Multi-ion conduction and selectivity in the high conductance Ca^{++}-activated K^+ channel from skeletal muscle. *Biophysical Journal.* 50:1025–1034.

Fabiato, A. 1988. Computer program for calculating total from specified free or free from specified total ionic concentrations in aequeous solutions containing multiple metals and ligands. *Methods of Enzymology.* 157:378–416.

Franke, C., H. Hatt, and J. Dudel. 1987. Liquid filament switch for ultra-fast exchanges of solutions at excised patches of synaptic membrane of crayfish muscle. *Neuroscience Letters.* 77:199–204.

Golowasch, J., A. Kirkwood, and C. Miller. 1986. Allosteric effects of Mg^{2+} on the gating of Ca^{2+} activated K⁺ channels from mammalian skeletal muscle. *Journal of Experimental Biology.* 124:5–13.

Grygorczyk, R. 1987. Temperature dependence of Ca^{2+} activated K⁺ currents in the membrane of human erythrocytes. *Biochimica and Biophysica Acta.* 902:159–168.

Gurney, A. M., R. Y. Tsien, and H. A. Lester. 1987. Activation of a potassium current by rapid photochemically generated step increase of intracellular calcium in rat sympathetic neurons. *Proceedings of the National Academy of Sciences, USA.* 84:3496–3500.

Haylett, D. G., and D. H. Jenkinson. 1990. Calcium-activated potassium channels. *In* Potassium Channels. N. S. Cook, editor. Ellis Horwood Ltd., Chichester, UK. 70–95.

Hille, B. 1984. Ionic channels of excitable membranes. Sinauer Associates, Inc., Sunderland, MA. 256.

Hodgkin, A. L., and A. F. Huxley. 1952. A quantitative description of membrane current and its application to conduction and excitation in nerve. *Journal of Physiology.* 117:500–544.

Horn, R. 1987. Statistical methods for model discrimination. *Biophysical Journal.* 51:255–263.

Ikemoto, Y., K. Ono, A. Yoshida, and N. Akaike. 1989. Delayed activation of large-conductance Ca^{2+}-activated K channels in hippocampal neurons of the rat. *Biophysical Journal.* 56:207–212.

Isenberg, G., and U. Klöckner. 1982. Calcium tolerant ventricular myocytes prepared by preincubation in a 'KB medium'. *Pflügers Archiv.* 395:6–18.

Klöckner, U., and G. Isenberg. 1985. Action potentials and net membrane current of isolated smooth muscle cells (urinary bladder of the guinea-pig). *Pflügers Archiv.* 405:329–339.

Latorre, R., R. Coronado, and C. Vergara. 1984. K⁺ channels gated by voltage and ions. *Annual Review of Physiology.* 46:485–495.

Latorre, R., A. Oberhauser, P. Labarca, and O. Alvarez. 1989. Varieties of calcium-activated potassium channels. *Annual Review of Physiology.* 51:385–399.

Magleby, K. L., and B. S. Pallotta. 1983a. Calcium dependence of open and shut interval distributions from calcium-activated potassium channels in cultured rat muscle. *Journal of Physiology.* 344:585–604.

Magleby, K. L., and B. S. Pallotta. 1983b. Burst kinetics of single calcium-activated potassium channels in cultured rat muscle. *Journal of Physiology.* 344:605–623.

Markwardt, F., and G. Isenberg. 1990. Ca^{2+}-dependent activation of maxi K⁺-channels studied by fast concentration jumps in inside-out patches of myocytes from guinea-pig urinary bladder. *Journal of Physiology.* 430:120P. (Abstr.)

Markwardt, F., and G. Isenberg. 1991. Activation of maxi K⁺-channels by Ca^{2+}-concentration jumps in myocytes of guinea-pig urinary bladder. *Pflügers Archiv.* 418:R48. (Abstr.)

Marty, A. 1989. The physiological role of calcium-dependent channels. *Trends in Neurosciences.* 12:420–424.

McManus, O. B., and K. L. Magleby. 1988. Kinetic states and modes of single large-conductance calcium-activated potassium channels in cultured rat skeletal muscle. *Journal of Physiology.* 402:79–120.

McManus, O. B., and K. L. Magleby. 1989. Kinetic time constants independent of previous single channel activity suggest Markov gating for a large conductance Ca-activated K channel. *Journal of General Physiology.* 94:1037–1070.

Methfessel, C., and G. Boheim. 1982. The gating of single calcium-dependent potassium channels is described by an activation/blockade mechanism. *Biophysics of Structure and Mechanics*. 9:35–60.

Moczydlowski, E., and R. Latorre. 1983. Gating kinetics of Ca^{2+}-activated K^+-channel from rat muscle incorporated into planar lipid bilayers. *Journal of General Physiology*. 82:511–542.

Ruknudin, A., M. J. Song, and F. Sachs. 1991. The ultrastructure of patch-clamped membranes: a study using high voltage electron microscopy. *Journal of Cell Biology*. 112:125–131.

Villarroel, A., O. Alvarez, A. Oberhauser, and R. Latorre. 1988. Probing a Ca^{2+}-activated K^+ channel with quaternary ammonium ions. *Pflügers Archiv*. 413:118–126.

Woodhull, A. N. 1973. Ionic blockage of sodium channels in nerve. *Journal of General Physiology*. 61:687–708.